

Viscosity- and Hydrodynamic-Radius Expansion Factors of Oligo- and Poly(α -methylstyrene)s in Dilute Solution

Yumiko Tominaga, Ikuko Suda, Masashi Osa, Takenao Yoshizaki, and Hiromi Yamakawa*

Department of Polymer Chemistry, Kyoto University, Kyoto 606-8501, Japan

Received July 30, 2001; Revised Manuscript Received November 10, 2001

ABSTRACT: The intrinsic viscosity $[\eta]$ was determined for 23 samples of atactic oligo- and poly(α -methylstyrene)s (a-P α MS), each with the fraction of racemic diads $f_r = 0.72$, in the range of weight-average molecular weight M_w from 4.12×10^2 to 5.46×10^6 in three good solvents, toluene, 4-*tert*-butyltoluene, and *n*-butyl chloride, at 25.0 °C. The translational diffusion coefficient D was also determined from dynamic light-scattering measurements for 17 a-P α MS samples in the range of M_w from 1.04×10^3 to 3.22×10^6 under the same solvent conditions. It was found that the values of $[\eta]$ in toluene and *n*-butyl chloride are appreciably smaller than the previous ones of $[\eta]_\Theta$ in cyclohexane at 30.5 °C (Θ) in the oligomer region in which the intramolecular excluded-volume effect may be ignored, while those of $[\eta]$ in 4-*tert*-butyltoluene are only slightly larger than the latter there because of the dependence on solvent of the hydrodynamic chain (bead) diameter. The disagreement in toluene and *n*-butyl chloride may be regarded as arising from the so-called specific interaction between polymer and solvent molecules, and therefore the viscosity-radius expansion factor α_η in these solvents was calculated after removing its contribution. On the other hand, the values of the hydrodynamic radius R_H defined from D in the three good solvents were found to agree well with the previous ones of $R_{H,\Theta}$ in cyclohexane at Θ in the oligomer region, and therefore the hydrodynamic-radius expansion factor α_H could be calculated straightforwardly. It was then found that both plots of α_η and α_H against the scaled excluded-volume parameter \bar{z} for a-P α MS in the three good solvents along with those for atactic polystyrene and atactic and isotactic poly(methyl methacrylate)s previously studied form their respective single-composite curves, confirming the validity of the quasi-two-parameter scheme that all expansion factors are functions only of \bar{z} irrespective of the differences in polymer species (chain stiffness and local chain conformation) and solvent condition.

Introduction

In a previous paper,¹ we have reported results for the gyration-radius expansion factor α_S for the root-mean-square radius of gyration $\langle S^2 \rangle^{1/2}$ for atactic oligo- and poly(α -methylstyrene)s (a-P α MS) with the fraction of racemic diads $f_r = 0.72$ in three good solvents, toluene, 4-*tert*-butyltoluene, and *n*-butyl chloride, at 25.0 °C. From a comparison of these results with previous ones² for atactic polystyrene (a-PS) with $f_r = 0.59$, atactic poly(methyl methacrylate) (a-PMMA) with $f_r = 0.79$, and isotactic (i-) PMMA with $f_r \approx 0.01$, it has then been reconfirmed that the quasi-two-parameter (QTP) scheme² that all expansion factors are functions only of the scaled excluded-volume parameter \bar{z} irrespective of the differences in polymer species and solvent condition is valid for α_S for flexible polymers. Recall here that the a-P α MS chain has a strong helical nature like the a-PMMA chain, tending to retain large and clearly distinguishable helical portions in dilute solution.³ In this paper, we proceed to make a similar study of the viscosity- and hydrodynamic-radius expansion factors α_η and α_H for the cubic root of the intrinsic viscosity $[\eta]^{1/3}$ and the hydrodynamic radius R_H , the latter being defined from the translational diffusion coefficient D .

In our previous studies of the excluded-volume effects in dilute solutions of oligomers and polymers,^{2,4} attention has always been given to the agreement between the perturbed chain dimension in a good solvent and the unperturbed one in a Θ solvent adopted as a reference standard in the oligomer region in which the intramolecular excluded-volume effect may be ignored.

In the present case of a-P α MS, it has in fact been confirmed in the previous paper¹ that the values of $\langle S^2 \rangle$ in toluene at 25.0 °C and in 4-*tert*-butyltoluene at 25.0 °C agree well with that of $\langle S^2 \rangle_\Theta$ in cyclohexane at 30.5 °C (Θ)³ in the range of the weight-average degree of polymerization $x_w \lesssim 30$ or of the weight-average molecular weight $M_w \lesssim 3.5 \times 10^3$. We note that $\langle S^2 \rangle$ in this range could not be determined from small-angle X-ray scattering measurements in *n*-butyl chloride.¹

It is important to note that the above agreement between the values of $\langle S^2 \rangle$ and $\langle S^2 \rangle_\Theta$ for a-P α MS does not necessarily indicate the agreement between values of $[\eta]$ in the good solvents and that of $[\eta]_\Theta$ previously⁵ determined in the Θ solvent in the oligomer region. In anticipation of results, it should be mentioned here that values of $[\eta]$ in toluene at 25.0 °C and in *n*-butyl chloride at 25.0 °C, although not negative, are appreciably smaller than that⁵ of $[\eta]_\Theta$ in cyclohexane at Θ in the range of $x_w \lesssim 35$ or of $M_w \lesssim 4 \times 10^3$. This disagreement (or negative $[\eta]$) may be regarded as arising from the so-called specific interaction between polymer and solvent molecules such that a liquid structure of some kind existing in the solvent is destroyed in the vicinity of the polymer molecule.^{2,6,7} For a calculation of α_η , we then use the procedure previously^{2,6,7} adopted to remove its contribution to $[\eta]$. In contrast to the case of $[\eta]$ above, values of R_H for a-P α MS in the three good solvents agree well with that⁵ of $R_{H,\Theta}$ in cyclohexane at Θ . Note that the notion of the specific interaction does not exist in the case of D and R_H .

Table 1. Values of M_w , x_w , M_w/M_n , and f_r for Atactic Oligo- and Poly(α -methylstyrene)s

sample	M_w	x_w	M_w/M_n	f_r
OAMS3	4.12×10^2	3	1	0.73
OAMS5	6.48×10^2	5	<1.01	
OAMS6	7.66×10^2	6	<1.01	
OAMS7	8.84×10^2	7	<1.01	
OAMS8	1.04×10^3	8.29	1.01	
OAMS10	1.27×10^3	10.3	1.01	
OAMS13	1.60×10^3	13.1	1.02	0.71
OAMS19	2.27×10^3	18.7	1.07	0.72
OAMS25	2.96×10^3	24.6	1.06	0.72
OAMS33	3.95×10^3	33.0	1.04	0.72
OAMS38	4.57×10^3	38.2	1.07	0.72
OAMS67	7.97×10^3	67.1	1.04	0.72
AMS1	1.30×10^4	109	1.02	0.73
AMS2	2.48×10^4	209	1.02	0.73
AMS5	5.22×10^4	442	1.02	0.73
AMS6	6.46×10^4	547	1.03	0.72
AMS11	1.15×10^5	973	1.04	0.73
AMS15	1.46×10^5	1240	1.02	0.73
AMS24	2.38×10^5	2010	1.05	0.73
AMS40	4.07×10^5	3450	1.02	0.73
AMS80	8.50×10^5	7200	1.05	0.72
AMS200	2.06×10^6	17400	1.05	0.72
AMS320	3.22×10^6	27300	1.05	0.73
AMS550	5.46×10^6	46300		0.70

Experimental Section

Materials. All the a-PaMS samples used in this work are the same as those used in the previous studies^{1,3,5} of $\langle S^2 \rangle_\Theta$, $[\eta]_\Theta$, $R_{H,\Theta}$, and α_S , i.e., fractions separated by preparative gel permeation chromatography (GPC) or fractional precipitation from the original samples prepared by living anionic polymerization.^{1,8} We note that the sample AMS40 is a fraction from the commercial sample 20538-2 from Polymer Laboratories Ltd. We also note that the initiating chain end of each polymerized sample is a *sec*-butyl group and the other end is a hydrogen atom.

The values of M_w determined from ^1H and ^{13}C NMR spectra, by analytical GPC, or from (static) light scattering measurements (in cyclohexane at Θ),^{1,8} x_w estimated from M_w , f_r determined from ^1H and ^{13}C NMR spectra,^{1,8} and the ratio of M_w to the number-average molecular weight M_n determined by analytical GPC^{1,8} are given in Table 1. Although f_r of the samples OAMS5–OAMS10 could not be determined because of the complexity of their ^1H NMR spectra, they may be regarded as having almost the same value of f_r as OAMS3 or OAMS13 ($0.71 \leq f_r \leq 0.73$), since the seven samples OAMS3–OAMS13 are fractions from one original sample.⁸ As seen from the values of f_r , all the samples except AMS550 have the fixed stereochemical composition $f_r = 0.72 \pm 0.01$. Although the value 0.70 of f_r of AMS550 is somewhat smaller than those of the others, this difference may be considered to have no significant effect on solution properties.¹ As seen from the values of M_w/M_n , all the samples except AMS550 are very narrow in molecular weight distribution. Although the value of M_w/M_n for the sample AMS550 could not be determined with high accuracy because of the lack of the GPC calibration curve in the necessary range, its molecular weight distribution may be considered to be as narrow as that of the other samples.

The solvents cyclohexane, toluene, and *n*-butyl chloride were purified according to standard procedures. The solvent 4-*tert*-butyltoluene was purified by distillation under reduced pressure in a dried nitrogen atmosphere after refluxing over sodium.

Viscosity. Viscosity measurements were carried out in toluene at 25.0 °C, in 4-*tert*-butyltoluene at 25.0 °C, and in *n*-butyl chloride at 25.0 °C for the samples listed in Table 1 and also in cyclohexane at Θ for the sample AMS550. For the measurements, we used conventional capillary and four-bulb spiral capillary viscometers of the Ubbelohde type. The flow time was measured to a precision of 0.1 s, keeping the difference between those of the solvent and solution larger

than 20 s. The test solutions were maintained at constant temperature within ± 0.005 °C during the measurements.

The test solutions were prepared by continuous stirring at 50 °C for 3–7 days. The polymer mass concentrations c (in g/cm³) were calculated from the weight fractions with the densities of the solutions. The density of each solution was calculated with the partial specific volume v_2 of the polymer and the density ρ_0 of the solvent. The quantities v_2 and ρ_0 were measured with a pycnometer of the Lipkin–Davison type having the volume of 10 cm³. Density corrections were also made in the calculations of the relative viscosity η_r from the flow times of the solution and solvent. The data obtained for the specific viscosity η_{sp} and η_r in the range of $\eta_r < 1.7$ were treated as usual by the Huggins (η_{sp}/c vs c) and Fuoss–Mead [$\ln(\eta_r/c)$ vs c] plots, respectively, to determine $[\eta]$ and the Huggins coefficient K' . (Note that the two plots have the same intercept.)

Dynamic Light Scattering. Dynamic light scattering (DLS) measurements were carried out to determine D for the samples in toluene at 25.0 °C, in 4-*tert*-butyltoluene at 25.0 °C, and in *n*-butyl chloride at 25.0 °C by the use of a Brookhaven Instruments model BI-200SM light scattering goniometer with vertically polarized incident light of wavelength $\lambda_0 = 488$ nm from a Spectra-Physics model 2020 argon ion laser equipped with a model 583 temperature-stabilized etalon for a single-frequency-mode operation. The photomultiplier tube used was EMI 9863B/350, the output from which was processed by a Brookhaven Instruments model BI-9000AT digital correlator. (An electric shutter was attached to the original detector alignment in order to monitor the dark count automatically.) The normalized autocorrelation function $g^{(2)}(t)$ of scattered light intensity $I(t)$ at time t was measured at four or five concentrations and at scattering angles θ ranging from 18° to 40°. The most concentrated solution of each sample was prepared in the same manner as in the case of the viscosity measurements. It was optically purified by filtration through a Teflon membrane of pore size 0.45 or 0.10 μm . The solutions of lower concentrations were obtained by successive dilution. The polymer mass concentrations c were calculated from the weight fractions with the densities of the solutions.

From the data for $g^{(2)}(t)$ so determined at finite concentrations c , we determine D at an infinitely long time at infinite dilution in the same manner as that used in previous studies.⁹ At small c , the plot of $1/2 \ln[g^{(2)}(t) - 1]$ against t in general follows a straight line represented by

$$1/2 \ln[g^{(2)}(t) - 1] = \text{const} - At \quad (1)$$

with A the slope for such large t where all the internal motions of solute polymer chains have relaxed away.

With the slope A estimated from the plot, we may determine the apparent diffusion coefficient $D^{(\text{LS})}(c)$ at finite c from

$$D^{(\text{LS})}(c) = \lim_{k \rightarrow 0} A/k^2 \quad (2)$$

where k is the scattering vector and is given by

$$k = (4\pi/\tilde{\lambda}) \sin(\theta/2) \quad (3)$$

with $\tilde{\lambda}$ the wavelength of the incident light in the solvent. At very small c , $D^{(\text{LS})}(c)$ may be expanded as

$$D^{(\text{LS})}(c) = D^{(\text{LS})}(0)(1 + k_D^{(\text{LS})}c + \dots) \quad (4)$$

so that the desired $D = D(\infty)$ (at an infinitely long time) may be determined by an extrapolation of $D^{(\text{LS})}(c)$ to $c = 0$ as

$$D = D^{(\text{LS})}(0) \quad (5)$$

The values of the refractive index n_0 of toluene, 4-*tert*-butyltoluene, and *n*-butyl chloride at 25.0 °C and at $\lambda_0 = 488$ nm are 1.505₆, 1.499₅, and 1.404₇, respectively. The n_0 value of 4-*tert*-butyltoluene was measured by the use of an Abbe refractometer (ERMA OPTICAL WORKS). For the other

Table 2. Results of Viscometry for Atactic Oligo- and Poly(α -methylstyrene)s in Θ and Good Solvents

sample	cyclohexane, 30.5 °C (Θ)		toluene, 25.0 °C		4- <i>tert</i> -butyltoluene, 25.0 °C		<i>n</i> -butyl chloride, 25.0 °C	
	$[\eta]_{\Theta}$, dL/g	K	$[\eta]$, dL/g	K	$[\eta]$, dL/g	K	$[\eta]$, dL/g	K
OAMS3			0.0219	0.96				
OAMS5			0.0273	0.90				
OAMS6			0.0293	0.85			0.0298	0.87
OAMS7					0.0402	0.81		
OAMS8			0.0321	0.92				
OAMS10			0.0353	0.72			0.0344	0.88
OAMS13			0.0383	0.89	0.0489	0.85	0.0381	0.87
OAMS19			0.0429	0.87	0.0544	0.80	0.0435	0.80
OAMS25					0.0583	0.84	0.0472	0.87
OAMS33			0.0552	0.80	0.0639	0.83	0.0530	0.80
OAMS67			0.0800	0.60	0.0854	0.79	0.0734	0.75
AMS1			0.105	0.52				
AMS2			0.155	0.47	0.141	0.66	0.122	0.71
AMS5			0.250	0.40	0.201	0.64	0.182	0.63
AMS6			0.285	0.39				
AMS11			0.426	0.36				
AMS15			0.511	0.34	0.363	0.51	0.323	0.60
AMS24			0.689	0.37				
AMS40			0.999	0.35	0.623	0.36	0.571	0.48
AMS80			1.78	0.33	1.04	0.32	0.916	0.40
AMS200			3.20	0.31	1.81	0.32	1.58	0.42
AMS320			4.84	0.33	2.44	0.34	2.15	0.37
AMS550	1.60	0.68	6.75	0.30	3.54	0.34	3.00	0.39

solvents, n_0 was estimated by a linear interpolation of the plot of n_0 against λ_0^{-2} with literature values¹⁰ of n_0 at $\lambda_0 = 436$ and 546 nm, which are 1.5151 at 436 nm and 1.4980 at 546 nm for toluene and 1.4088 at 436 nm and 1.4014 at 546 nm for *n*-butyl chloride. The values of the viscosity coefficient η_0 of toluene, 4-*tert*-butyltoluene, and *n*-butyl chloride at 25.0 °C are 0.552, 1.111, and 0.427 cP, respectively.

Results

Intrinsic Viscosity. Intrinsic viscosity data obtained for the a-P α MS samples in toluene at 25.0 °C, in 4-*tert*-butyltoluene at 25.0 °C, and in *n*-butyl chloride at 25.0 °C are summarized in Table 2 along with the values of the Huggins coefficient K . There are also given the values of $[\eta]_{\Theta}$ and K for the sample AMS550 determined in the present work in cyclohexane at 30.5 °C (Θ). It is seen from the table that K for a-P α MS in each good solvent decreases with increasing M_w as in the previous case of the Θ solvent⁵ and also in the cases of a-PS^{11,12} and a- and i-PMMA^{13,14} in their respective good solvents.

Figure 1 shows double-logarithmic plots of $[\eta]/M_w^{1/2}$ ($[\eta]$ in dL/g) against M_w for a-P α MS. The unfilled, bottom-half-filled, and top-half-filled circles represent the values in toluene at 25.0 °C, in 4-*tert*-butyltoluene at 25.0 °C, and in *n*-butyl chloride at 25.0 °C, respectively. The filled circles represent the previous values⁵ and the present one for the sample AMS550 (with the largest M_w) in cyclohexane at Θ . The solid curve connects smoothly the data points in each solvent.

The most remarkable feature to note in Figure 1 is that the data points in toluene at 25.0 °C and in *n*-butyl chloride at 25.0 °C deviate appreciably downward from those in cyclohexane at Θ in the range of $M_w \lesssim 4 \times 10^3$, in which the intramolecular excluded-volume effect may be ignored and in which the difference between them was therefore expected to be small if any. In fact, the value of $\langle S^2 \rangle$ in toluene at 25.0 °C agrees well with that of $\langle S^2 \rangle_{\Theta}$ in cyclohexane at Θ in the oligomer region.¹ As mentioned in the Introduction and explicitly shown in the next (Discussion) section, the above disagreement for $[\eta]$ may be regarded as arising from the specific interaction between polymer and solvent molecules.^{2,6,7} On the other hand, the data points in 4-*tert*-butyltoluene

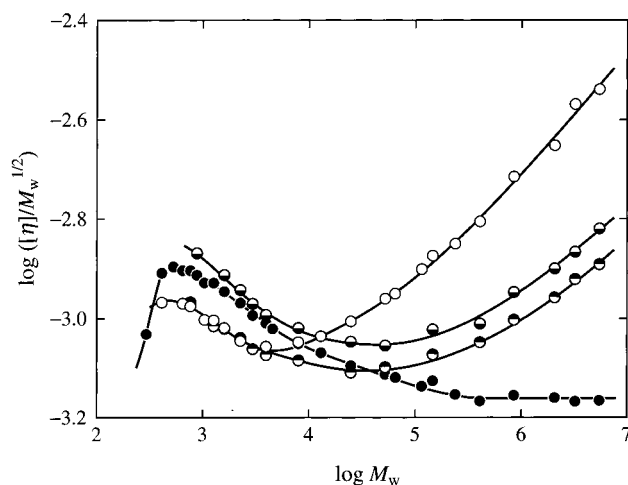


Figure 1. Double-logarithmic plots of $[\eta]/M_w^{1/2}$ ($[\eta]$ in dL/g) against M_w for a-P α MS: (○) present data in toluene at 25.0 °C; (◐) present data in 4-*tert*-butyltoluene at 25.0 °C; (◑) present data in *n*-butyl chloride at 25.0 °C; (●) previous⁵ and present data in cyclohexane at 30.5 °C (Θ). The solid curve connects smoothly the data points in each solvent.

at 25.0 °C deviate only slightly upward from those in cyclohexane at Θ in the same range of M_w . We note that the value of $\langle S^2 \rangle$ in 4-*tert*-butyltoluene at 25.0 °C also agrees well with that of $\langle S^2 \rangle_{\Theta}$ in cyclohexane at Θ in the oligomer region.¹ There is no appreciable effect of specific interaction in 4-*tert*-butyltoluene. The small difference between the value of $[\eta]$ in this solvent and that of $[\eta]_{\Theta}$ in the oligomer region may rather be regarded as arising from that between values of the hydrodynamic chain (bead) diameter as in the case of a- and i-PMMA^{2,13,14} since it becomes definitely smaller with increasing M_w there. As M_w is increased from ca. 10^4 , the data points in all the good solvents deviate upward progressively from those in cyclohexane at Θ because of the excluded-volume effect.

As clearly seen from Figure 1, it is inadequate to calculate α_{η} in toluene at 25.0 °C and in *n*-butyl chloride at 25.0 °C directly from the observed values of $[\eta]$, so that a proper correction is introduced in the Discussion to remove the contribution of the specific interaction.

Table 3. Results of DLS Measurements for Atactic Oligo- and Poly(α -methylstyrene)s in Good Solvents

sample	toluene, 25.0 °C			4- <i>tert</i> -butyltoluene, 25.0 °C			<i>n</i> -butyl chloride, 25.0 °C		
	$10^7 D$, cm ² /s	$k_D^{(LS)}$, cm ³ /g	R_H , Å	$10^7 D$, cm ² /s	$k_D^{(LS)}$, cm ³ /g	R_H , Å	$10^7 D$, cm ² /s	$k_D^{(LS)}$, cm ³ /g	R_H , Å
OAMS8							70.0	-1.7	7.31
OAMS19	35.9	-0.75	11.0						
OAMS25	31.6	-0.72	12.5						
OAMS33	27.4	-0.36	14.4						
OAMS38	25.8	-0.71	15.3	12.5	-3.9	15.7	35.2	-2.5	14.5
OAMS67	19.0	0.63	20.8						
AMS1	14.9	1.7	26.6	7.46	-4.1	26.3	19.8	-3.3	25.8
AMS2	10.8	3.9	36.6						
AMS5	7.25	9.6	54.6	3.80	-4.2	51.8	10.1	-4.2	50.5
AMS6	6.34	11	62.4						
AMS11	4.55	22	87.0						
AMS15	4.04	26	97.9	2.22	-1.6	88.7	5.94	-4.2	86.1
AMS24	3.08	39	128	1.72	2.3	114	4.65	0.0	110
AMS40	2.33	64	170				3.59	9.2	143
AMS80	1.49	110	266	0.878	18	224	2.37	11	216
AMS200	0.912	190	434	0.553	49	355	1.48	46	347
AMS320	0.706	260	560	0.425	64	463	1.13	52	453

As for α_η in 4-*tert*-butyltoluene at 25.0 °C, the data in the oligomer region (for $M_w \lesssim 3 \times 10^3$) are omitted as in the case of a- and i-PMMA^{2,13,14} (see the Discussion).

In the present paper, we do not compare the present data with literature ones,^{15–18} since none of the latter cover the oligomer region.

Translational Diffusion Coefficient. The data points for $\frac{1}{2} \ln[g^{(2)}(t) - 1]$ as a function of t directly obtained from the DLS measurements for each test solution at each scattering angle θ were found to follow a straight line as given by eq 1, so that the slope A could be unambiguously determined. Furthermore, in the range of k (or θ) in which the DLS measurements were carried out, the ratio A/k^2 was found to be independent of k within experimental error for all the test solutions. Then $D^{(LS)}(c)$ for each solution was calculated from eq 2 as a mean of observed values of A/k^2 over k . Finally, values of $D^{(LS)}(c)$ so obtained for each sample in each solvent were plotted against c in order to estimate $D^{(LS)}(0)$ at infinite dilution. Although the plots are not explicitly shown here, the data points for each sample in each solvent followed a straight line, and therefore $D^{(LS)}(0)$ and $k_D^{(LS)}$ in eq 4 could be accurately determined from its ordinate intercept and slope, respectively. With the values of $D [=D^{(LS)}(0)]$ so determined, we may calculate the hydrodynamic radius R_H for each sample in each solvent from

$$R_H = k_B T / 6\pi\eta_0 D \quad (6)$$

where k_B is the Boltzmann constant, T is the absolute temperature, and η_0 is the viscosity coefficient of the solvent. The values of D , $k_D^{(LS)}$, and R_H so obtained for a-P α MS in toluene at 25.0 °C, in 4-*tert*-butyltoluene at 25.0 °C, and in *n*-butyl chloride at 25.0 °C are given in Table 3. As in the cases of a-PS^{19,20} and a- and i-PMMA^{21–23} $k_D^{(LS)}$ for a-P α MS in each good solvent increases from negative to positive values with increasing M_w in contrast to the results in the Θ solvent.⁵ We note that DLS measurements have not been carried out for the sample AMS550 (with the largest M_w), since the contribution of internal motions to $g^{(2)}(t)$ is considered to be so large that an accurate determination of the slope A becomes difficult.

Figure 2 shows double-logarithmic plots of $R_H/M_w^{1/2}$ (R_H in Å) against M_w . The unfilled, bottom-half-filled, and top-half-filled circles represent the values in toluene at 25.0 °C, in 4-*tert*-butyltoluene at 25.0 °C, and in

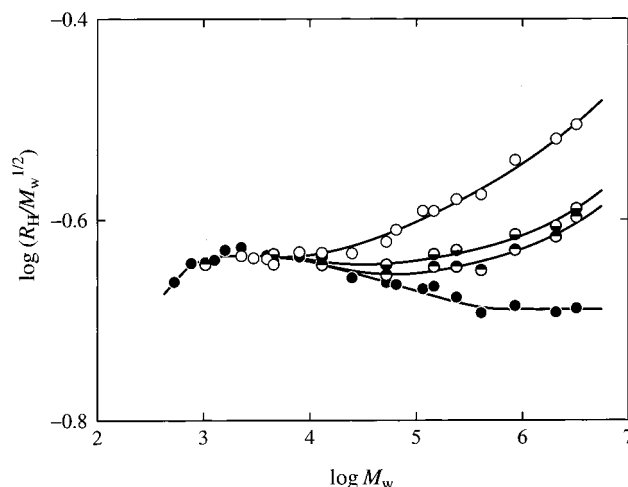


Figure 2. Double-logarithmic plots of $R_H/M_w^{1/2}$ (R_H in Å) against M_w for a-P α MS. The symbols have the same meaning as those in Figure 1. The solid curve connects smoothly the data points in each solvent.

n-butyl chloride at 25.0 °C, respectively. The filled circles represent the previous values⁵ in cyclohexane at Θ . The solid curve connects smoothly the data points in each solvent.

In contrast to the case of $[\eta]$, the data points in all the good solvents agree well with those in cyclohexane at Θ in the range of $M_w \lesssim 4 \times 10^3$ within experimental error and then deviate upward progressively from the latter with increasing M_w in the range of $M_w \gtrsim 4 \times 10^3$ because of the excluded-volume effect. Such behavior of the plots is very similar to that of $\langle S^2 \rangle/x_w$ and $\langle S^2 \rangle_\Theta/x_w$ for a-P α MS shown in Figure 1 of ref 1, although the corresponding data points for $\langle S^2 \rangle/x_w$ in *n*-butyl chloride in the oligomer region are lacking. The results are consistent with the ones for a-PS²⁰ and a- and i-PMMA²³. For a-P α MS, therefore, we may straightforwardly calculate α_H by adopting $R_{H,\Theta}$ in the Θ solvent as the unperturbed value $R_{H,0}$ in each good solvent as in the previous case of α_S ¹ and also in the case of α_H for the above polymers.^{20,23} In this connection, we note that in the case of R_H there is no need to consider the specific interaction² and that the possible difference between R_H values in different solvents in the oligomer region may be regarded as arising from that between values of the hydrodynamic chain diameter as in the case of poly-(dimethylsiloxane).^{2,7}

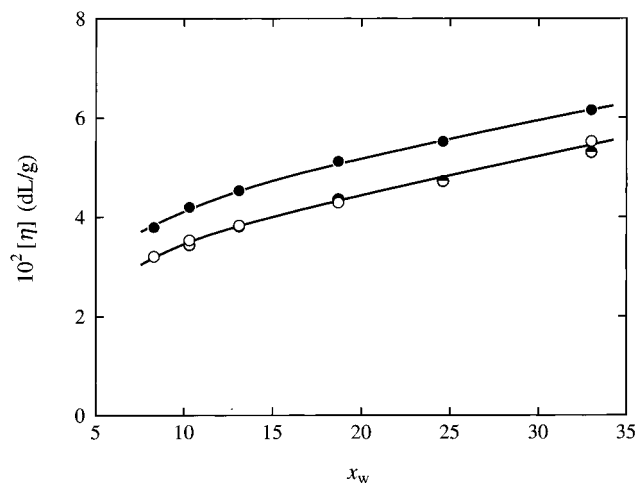


Figure 3. Plots of $[\eta]$ against x_w for a-PaMS oligomers. The symbols have the same meaning as those in Figure 1. The solid curve connects smoothly the data points in each solvent.

We do not compare the present data with those determined from literature values of D or the sedimentation coefficient^{17,18,24–27} for the same reason as that in the case of $[\eta]$.

Discussion

Viscosity-Radius Expansion Factor. There are three possible sources of the difference between the unperturbed value $[\eta]_0$ of $[\eta]$ in a good solvent and $[\eta]_\Theta$ in a Θ solvent for a given polymer whose $\langle S^2 \rangle_0$ and $\langle S^2 \rangle_\Theta$ in the respective solvents agree well with each other.² They are the specific interaction, the dependence on solvent of the hydrodynamic chain diameter, and the dependence on solvent of the Flory–Fox factor. The relative contributions of the first two decrease with increasing M_w and vanish asymptotically in the limit of $M_w \rightarrow \infty$, while the third contribution remains over the whole range of M_w . In the present case of a-PaMS, the third source is irrelevant, as shown later, so that we examine which of the first two causes the above-observed difference between $[\eta]$ in toluene at 25.0 °C or in *n*-butyl chloride at 25.0 °C and $[\eta]_\Theta$ in cyclohexane at 30.5 °C (Θ) in the oligomer region.

As discussed rather in detail in section 6.5.3 of ref 2, the contribution of the specific interaction may be represented by an empirical additional nonpositive term²⁸ η^* independent of x_w (or M_w) in $[\eta]$. If it exists and if the hydrodynamic chain diameters for a-PaMS in the three solvents are the same, then the difference between the value of $[\eta]$ in each of the two good solvents and that of $[\eta]_\Theta$ in cyclohexane at Θ must become a constant independent of x_w in the oligomer region in which the intramolecular excluded-volume effect may be ignored. Note that the difference depends on x_w if the hydrodynamic chain diameters are different, as already mentioned. Figure 3 shows plots of $[\eta]$ against x_w for a-PaMS in toluene at 25.0 °C (unfilled circles), in *n*-butyl chloride at 25.0 °C (top-half-filled circles), and in cyclohexane at Θ (filled circles) in the oligomer region. The solid curve connects smoothly the data points in each solvent. Here, we have drawn the single curve common to the data points in the two good solvents, since there is no appreciable difference between them. It is clearly seen that the difference between $[\eta]$ in the two good solvents and $[\eta]_\Theta$ in the Θ solvent is in fact independent of x_w in the oligomer region within experi-

Table 4. Values of α_η^3 of Atactic Oligo- and Poly(α -methylstyrene)s in Good Solvents

sample	α_η^3		
	toluene, 25.0 °C	4- <i>tert</i> -butyltoluene, 25.0 °C	<i>n</i> -butyl chloride, 25.0 °C
OAMS8	1.04		
OAMS10	1.02		0.99 ₃
OAMS13	1.01		1.00
OAMS19	0.98 ₁		0.99 ₄
OAMS25			0.98 ₈
OAMS33	1.02	1.04	0.98 ₀
OAMS67	1.10	1.08	1.02
AMS1	1.16		
AMS2	1.29	1.12	1.03
AMS5	1.46	1.14	1.08
AMS6	1.51		
AMS11	1.75		
AMS15	1.82	1.28	1.16
AMS24	2.03		
AMS40	2.32	1.43	1.33
AMS80	2.77	1.61	1.43
AMS200	3.23	1.82	1.60
AMS320	3.97	2.00	1.77
AMS550	4.22	2.21	1.88

mental error. It may then be concluded that this difference in $[\eta]$ in the oligomer region arises just from the specific interaction.

If we assume that there is no contribution of the specific interaction to $[\eta]_\Theta$, α_η in the two good solvents may be calculated from^{2,6}

$$[\eta] - \eta^* = [\eta]_0 \alpha_\eta^3 \quad (7)$$

with $[\eta]_0 = [\eta]_\Theta$ and $\eta^* = -0.0073$ dL/g, where η^* has been estimated as a mean of differences between the values of $[\eta]$ and $[\eta]_\Theta$ shown in Figure 3. Recall that the previous analysis⁵ of $[\eta]_\Theta$ on the above assumption gives the satisfactory result. As already mentioned, we calculate α_η in 4-*tert*-butyltoluene at 25.0 °C from eq 7 with $[\eta]_0 = [\eta]_\Theta$ and $\eta^* = 0$ only for the samples with $M_w \gtrsim 3 \times 10^3$, for which the dependence on solvent of the hydrodynamic chain diameter may be neglected.

The values of α_η^3 so calculated for the a-PaMS samples in toluene at 25.0 °C, in 4-*tert*-butyltoluene at 25.0 °C, and in *n*-butyl chloride at 25.0 °C are given in Table 4. We note that the contribution of η^* to α_η becomes vanishingly small with increasing M_w for $M_w \gtrsim 10^5$.

Before proceeding to examine the behavior of α_η , we make brief mention of the QTP scheme or the Yamakawa–Stockmayer–Shimada (YSS) theory.² As already mentioned in the Introduction, on the basis of the helical wormlike (HW) chain model,² it claims that all the expansion factors α_S , α_η , and α_H are functions only of the scaled excluded-volume parameter \tilde{z} defined by

$$\tilde{z} = {}^3/{}_4 K(\lambda L) z \quad (8)$$

where z is the conventional excluded-volume parameter appearing in the two-parameter (TP) theory²⁹ and is defined by

$$z = (3/2\pi)^{3/2} (\lambda B) (\lambda L)^{1/2} \quad (9)$$

with λ^{-1} the stiffness parameter, B the excluded-volume strength, and L the total contour length of the HW chain. We note that B may be written in terms of the binary-cluster integral β between beads, their spacing a , and the differential-geometrical curvature κ_0 and

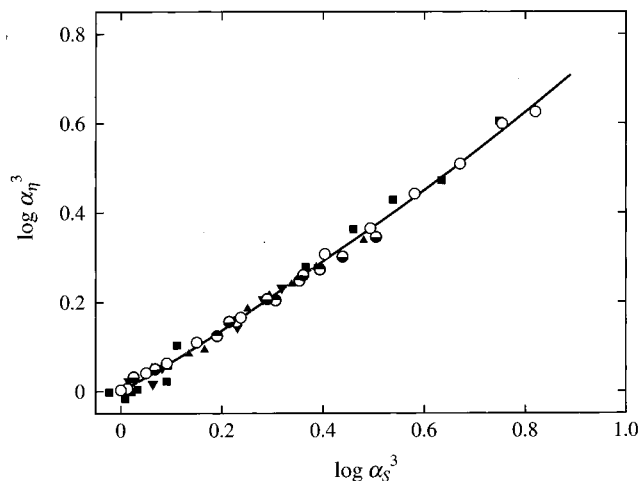


Figure 4. Double-logarithmic plots of α_η^3 against α_S^3 : (○) present data for a-PaMS in toluene at 25.0 °C; (◐) present data for a-PaMS in 4-*tert*-butyltoluene at 25.0 °C; (◑) present data for a-PaMS in *n*-butyl chloride at 25.0 °C; (■) a-PS in toluene at 15.0 °C;¹¹ (▲) a-PMMA in acetone at 25.0 °C;¹³ (▼) i-PMMA in acetone at 25.0 °C.¹⁴ The solid curve represents the QTP (or YSS) theory values calculated from eq 11 with eq 14 (see text).

torsion τ_0 of the characteristic helix, along with λ^{-1} . We omit here the explicit expression for B , since it is unnecessary for the following discussion. In eq 8, the coefficient $K(L)$ is given by

$$K(L) = \frac{4}{3} - 2.711L^{-1/2} + \frac{7}{6}L^{-1} \quad \text{for } L > 6$$

$$= L^{-1/2} \exp(-6.611L^{-1} + 0.9198 + 0.03516L) \quad \text{for } L \leq 6 \quad (10)$$

It is seen from eq 8 with eq 10 that $\tilde{z} = z$ in the limit of $\lambda L \rightarrow \infty$ (random-coil limit), so that the QTP theory becomes identical with the TP theory in this limit.

Now α_η may in general be written in the form²

$$\alpha_\eta = \alpha_\eta^{(0)} h_\eta \quad (11)$$

where h_η represents a possible effect of fluctuating hydrodynamic interaction and $\alpha_\eta^{(0)}$ is an appropriate function derived without its consideration. We note that both $\alpha_\eta^{(0)}$ and h_η are functions only of \tilde{z} in the QTP scheme, while $\alpha_\eta^{(0)}$ is a function only of z and $h_\eta = 1$ in the conventional TP theory. As usual,² we adopt the Barrett equation³⁰ for $\alpha_\eta^{(0)}$,

$$\alpha_\eta^{(0)} = (1 + 3.8\tilde{z} + 1.9\tilde{z}^2)^{0.1} \quad (12)$$

Since there is no available theory of h_η at the present time, we simply put

$$h_\eta = 1 \quad (13)$$

as in the case of the TP theory.

We first examine the relation between α_η and α_S . Figure 4 shows double-logarithmic plots of α_η^3 against α_S^3 for a-PaMS in toluene at 25.0 °C (unfilled circles), in 4-*tert*-butyltoluene at 25.0 °C (bottom-half-filled circles), and in *n*-butyl chloride at 25.0 °C (top-half-filled circles). For comparison, it also includes the values previously determined for a-PS in toluene at 15.0 °C (filled squares),¹¹ a-PMMA in acetone at 25.0 °C (filled

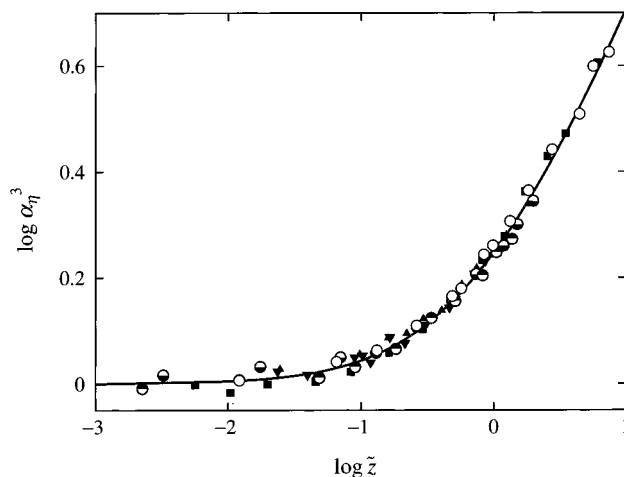


Figure 5. Double-logarithmic plots of α_η^3 against \tilde{z} . The symbols have the same meaning as those in Figure 4. The solid curve represents the QTP (or YSS) theory values calculated from eq 11 (see text).

triangles),¹³ and i-PMMA in acetone at 25.0 °C (inverted filled triangles).¹⁴ We note that the dependence on solvent of the Flory–Fox factor has been taken into account in the determination of α_η for a- and i-PMMA.^{2,13,14} The solid curve represents the QTP theory values calculated from eq 11 for α_η with the Domb–Barrett equation³¹ for α_S ,

$$\alpha_S^2 = [1 + 10\tilde{z} + (70\pi/9 + 10/3)\tilde{z}^2 + 8\pi^{3/2}\tilde{z}^3]^{2/15} \times [0.933 + 0.067 \exp(-0.85\tilde{z} - 1.39\tilde{z}^2)] \quad (14)$$

It is seen that the present data points for a-PaMS in the three different good solvents along with those for a-PS and a- and i-PMMA form a single-composite curve and that all the data points are well fitted by the theoretical curve. If the Flory–Fox factor for a-PaMS were dependent on solvent, the plots for it in the three good solvents would split as in the case of a- and i-PMMA.^{2,13,14} Thus, we have not considered the dependence on solvent of the Flory–Fox factor for a-PaMS.

Figure 5 shows double-logarithmic plots of α_η^3 against \tilde{z} with the same data as those in Figure 4. Here, values of \tilde{z} for a-PaMS have been calculated from eq 8 with eq 9 with $\lambda B = 0.43, 0.12$, and 0.080 previously determined from an analysis of α_S in toluene at 25.0 °C, in 4-*tert*-butyltoluene at 25.0 °C, and in *n*-butyl chloride at 25.0 °C, respectively, $\lambda^{-1} = 46.8$ Å, and values of L calculated from $L = M_w/M_L$ with the value 39.8 Å⁻¹ of the shift factor M_L as defined as the molecular weight per unit contour length. The values of λ^{-1} and M_L were previously determined from an analysis of $\langle S^2 \rangle_\Theta$.³ We note that values of \tilde{z} for a-PS¹¹ have been recalculated by the use of the values of the HW model parameters determined for a-PS from an analysis of $\langle S^2 \rangle_\Theta$,² corresponding to the above calculations for a-PaMS and the previous ones for a- and i-PMMA.^{13,14} The solid curve represents the QTP theory values calculated from eq 11. It is seen that the present data points for a-PaMS in the three different good solvents along with those for a-PS and a- and i-PMMA form a single-composite curve, indicating that the QTP scheme is valid for α_η as well as for α_S . It is also seen that all the data points are well fitted by the theoretical curve.

Hydrodynamic-Radius Expansion Factor. As mentioned in the Results section, α_H in the three good

Table 5. Values of α_H of Atactic Oligo- and Poly(α -methylstyrene)s in Good Solvents

sample	α_H		
	toluene, 25.0 °C	4- <i>tert</i> -butyltoluene, 25.0 °C	<i>n</i> -butyl chloride, 25.0 °C
OAMS8			0.99 ₅
OAMS19	0.98 ₄		
OAMS25	1.00		
OAMS33	0.99 ₆		1.00
OAMS38	0.98 ₉	1.01	
OAMS67	1.01		
AMS1	1.03	1.02	0.99 ₇
AMS2	1.06		
AMS5	1.10	1.04	1.02
AMS6	1.14		
AMS11	1.20		
AMS15	1.19	1.08	1.05
AMS24	1.25	1.11	1.07
AMS40	1.32		1.11
AMS80	1.40	1.18	1.14
AMS200	1.49	1.22	1.19
AMS320	1.52	1.26	1.23

solvents may be straightforwardly calculated from

$$R_H = R_{H,0}\alpha_H \quad (15)$$

with $R_{H,0} = R_{H,\Theta}$. The values of α_H so calculated for the a-P α MS samples in toluene at 25.0 °C, in 4-*tert*-butyltoluene at 25.0 °C, and in *n*-butyl chloride at 25.0 °C are given in Table 5.

Corresponding to the theoretical expression for α_η given in the last subsection, α_H may be written in the form²

$$\alpha_H = \alpha_H^{(0)} h_H \quad (16)$$

where we use the Barrett equation³² for $\alpha_H^{(0)}$,

$$\alpha_H^{(0)} = (1 + 5.93\bar{z} + 3.59\bar{z}^2)^{0.1} \quad (17)$$

and h_H is given by³³

$$h_H = \frac{0.88}{1 - 0.12\alpha_S^{-0.43}} \quad (18)$$

with α_S given by eq 14. We note that in eq 17 the coefficient 5.93 of \bar{z} has been adopted in place of the coefficient 6.09 originally adopted by Barrett.²

Figure 6 shows double-logarithmic plots of α_H against α_S for a-P α MS in toluene at 25.0 °C (unfilled circles), in 4-*tert*-butyltoluene at 25.0 °C (bottom-half-filled circles), and in *n*-butyl chloride at 25.0 °C (top-half-filled circles). As in Figure 4, it also includes the values previously determined for a-PS in toluene at 15.0 °C (filled squares),²⁰ a-PMMA in acetone at 25.0 °C (filled triangles),²³ and i-PMMA in acetone at 25.0 °C (inverted filled triangles).²³ The solid curve represents the QTP theory values calculated from eq 16 for α_H with eq 14 for α_S , and the dotted curve represents those of $\alpha_H^{(0)}$ calculated from eq 17 with eq 14. It is seen that the present data points for a-P α MS in the three different good solvents along with those for a-PS and a- and i-PMMA form a single-composite curve but deviate downward from the dotted curve and even from the solid curve. As already mentioned,² the disagreement between theory and experiment indicates that eq 18 for h_H underestimates the effect of fluctuating hydrodynamic interaction.

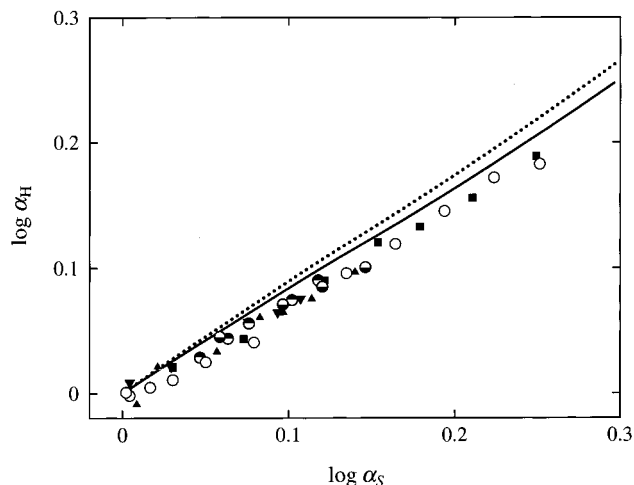


Figure 6. Double-logarithmic plots of α_H against α_S : (○) present data for a-P α MS in toluene at 25.0 °C; (◐) present data for a-P α MS in 4-*tert*-butyltoluene at 25.0 °C; (◑) present data for a-P α MS in *n*-butyl chloride at 25.0 °C; (■) previous data for a-PS in toluene at 15.0 °C;²⁰ (▲) previous data for a-PMMA in acetone at 25.0 °C;²³ (▼) previous data for i-PMMA in acetone at 25.0 °C.²³ The solid curve represents the QTP (or YSS) theory values calculated from eq 16 with eq 14, and the dotted curve those of $\alpha_H^{(0)}$ calculated from eq 17 with eq 14 (see text).

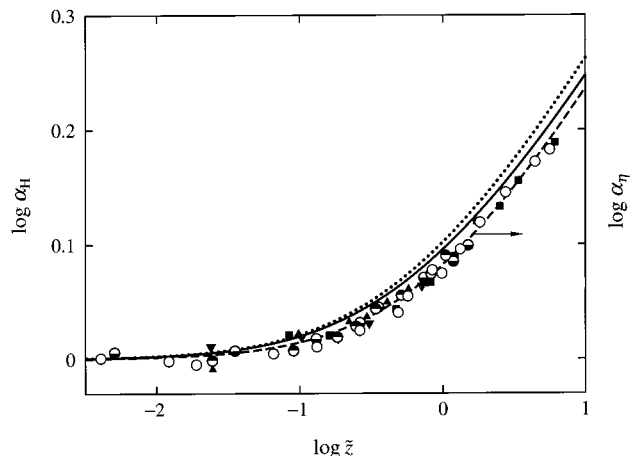


Figure 7. Double-logarithmic plots of α_H against \bar{z} . The symbols have the same meaning as those in Figure 6. The solid curve represents the QTP (or YSS) theory values calculated from eq 16, the dotted curve those of $\alpha_H^{(0)}$ calculated from eq 17, and the dashed curve those of α_η calculated from eq 11 (see text).

Figure 7 shows double-logarithmic plots of α_H against \bar{z} with the same data as those in Figure 6, where values of \bar{z} for a-P α MS have been calculated in the same manner as that in the above case of α_η . The solid curve represents the QTP theory values calculated from eq 16, and the dotted curve represents those of $\alpha_H^{(0)}$ calculated from eq 17. It is seen that the present data points for a-P α MS in the three different good solvents along with those for a-PS and a- and i-PMMA form a single-composite curve, indicating that the QTP scheme is valid for α_H as well as for α_S and α_η . As already mentioned,² the data points closely follow the dashed curve which represents the theoretical values of α_η calculated from eq 11, and therefore coincide accidentally with the data points for α_η within experimental error. The results are consistent with the Monte Carlo data.^{2,34}

Concluding Remarks

We have made a study of the viscosity- and hydrodynamic-radius expansion factors α_η and α_H as functions of the scaled excluded-volume parameter \bar{z} for a-P α MS with $f_i = 0.72$ in the three good solvents, toluene, 4-*tert*-butyltoluene, and *n*-butyl chloride, at 25.0 °C. It has been found that the values of $[\eta]$ in toluene and *n*-butyl chloride are appreciably smaller than those of $[\eta]_\Theta$ in cyclohexane at Θ in the oligomer region in which the intramolecular excluded-volume effect may be ignored, while those of $[\eta]$ in 4-*tert*-butyltoluene are only slightly larger than the latter there because of the dependence on solvent of the hydrodynamic chain diameter. The above disagreement in toluene and *n*-butyl chloride may be regarded as arising from the specific interaction between polymer and solvent molecules, and therefore α_η in these solvents has been calculated after removing its contribution. On the other hand, the values of R_H in the three good solvents have been found to agree well with those of $R_{H,\Theta}$ in cyclohexane at Θ in the oligomer region, and therefore α_H has been able to be straightforwardly calculated. It has then been shown that both plots of α_η and α_H against \bar{z} for a-P α MS in the three good solvents along with those for a-PS and a- and i-PMMA form their respective single-composite curves, confirming the validity of the QTP scheme that all the expansion factors (α_S , α_η , and α_H) are functions only of \bar{z} irrespective of the differences in polymer species (chain stiffness and local chain conformation) and solvent condition. We proceed to make a study of the second virial coefficient in forthcoming papers.

References and Notes

- (1) Osa, M.; Ueno, Y.; Yoshizaki, T.; Yamakawa, H. *Macromolecules* **2001**, *34*, 6402.
- (2) Yamakawa, H. *Helical Wormlike Chains in Polymer Solutions*; Springer: Berlin, 1997.
- (3) Osa, M.; Yoshizaki, T.; Yamakawa, H. *Macromolecules* **2000**, *33*, 4828.
- (4) Abe, F.; Einaga, Y.; Yoshizaki, T.; Yamakawa, H. *Macromolecules* **1993**, *26*, 1884 and succeeding papers.
- (5) Suda, I.; Tominaga, Y.; Osa, M.; Yoshizaki, T.; Yamakawa, H. *Macromolecules* **2000**, *33*, 9322.
- (6) Abe, F.; Einaga, Y.; Yamakawa, H. *Macromolecules* **1991**, *24*, 4423.
- (7) Horita, K.; Sawatari, N.; Yoshizaki, T.; Einaga, Y.; Yamakawa, H. *Macromolecules* **1995**, *28*, 4455 and references cited therein.
- (8) Osa, M.; Sumida, M.; Yoshizaki, T.; Yamakawa, H.; Ute, K.; Kitayama, T.; Hatada, K. *Polym. J.* **2000**, *32*, 361.
- (9) See, for example: Konishi, T.; Yoshizaki, T.; Yamakawa, H. *Macromolecules* **1991**, *24*, 5614.
- (10) Johnson, B. L.; Smith, J. In *Light Scattering from Polymer Solutions*; Huglin, M. B., Ed.; Academic Press: London, 1972; Chapter 2.
- (11) Abe, F.; Einaga, Y.; Yamakawa, H. *Macromolecules* **1993**, *26*, 1891.
- (12) Horita, K.; Abe, F.; Einaga, Y.; Yamakawa, H. *Macromolecules* **1993**, *26*, 5067.
- (13) Abe, F.; Horita, K.; Einaga, Y.; Yamakawa, H. *Macromolecules* **1994**, *27*, 725.
- (14) Kamijo, M.; Abe, F.; Einaga, Y.; Yamakawa, H. *Macromolecules* **1995**, *28*, 1095.
- (15) Noda, I.; Mizutani, K.; Kato, T.; Fujimoto, T.; Nagasawa, M. *Macromolecules* **1970**, *3*, 787.
- (16) Tsunashima, Y. Ph.D. Thesis, Kyoto University, 1972.
- (17) Lindner, J. S.; Wilson, W. W.; Mays, J. W. *Macromolecules* **1988**, *21*, 1, 3304.
- (18) Mays, J. W.; Nan, S.; Lewis, M. E. *Macromolecules* **1991**, *24*, 4857.
- (19) Yamada, T.; Yoshizaki, T.; Yamakawa, H. *Macromolecules* **1992**, *25*, 377.
- (20) Arai, T.; Abe, F.; Yoshizaki, T.; Einaga, Y.; Yamakawa, H. *Macromolecules* **1995**, *28*, 3609.
- (21) Dehara, K.; Yoshizaki, T.; Yamakawa, H. *Macromolecules* **1993**, *26*, 5137.
- (22) Sawatari, N.; Konishi, T.; Yoshizaki, T.; Yamakawa, H. *Macromolecules* **1995**, *28*, 1089.
- (23) Arai, T.; Sawatari, N.; Yoshizaki, T.; Einaga, Y.; Yamakawa, H. *Macromolecules* **1996**, *29*, 2309.
- (24) Noda, I.; Mizutani, K.; Kato, T. *Macromolecules* **1977**, *10*, 618.
- (25) Selser, J. C. *Macromolecules* **1981**, *14*, 346.
- (26) Cotts, P. M.; Selser, J. C. *Macromolecules* **1990**, *23*, 2050.
- (27) Kim, S. H.; Ramsay, D. J.; Patterson, G. D.; Selser, J. C. *J. Polym. Sci., Polym. Phys.* **1990**, *28*, 2023.
- (28) The word "nonnegative" below eq 6.134 of ref 2 should be replaced by "nonpositive".
- (29) Yamakawa, H. *Modern Theory of Polymer Solutions*; Harper & Row: New York, 1971. The electronic edition (<http://www.molsci.polym.kyoto-u.ac.jp/archives/redbook.pdf>) is available.
- (30) Barrett, A. J. *Macromolecules* **1984**, *17*, 1566.
- (31) Domb, C.; Barrett, A. J. *Polymer* **1976**, *17*, 179.
- (32) Barrett, A. J. *Macromolecules* **1984**, *17*, 1561.
- (33) Yamakawa, H.; Yoshizaki, T. *Macromolecules* **1995**, *28*, 3604.
- (34) Yoshizaki, T.; Yamakawa, H. *J. Chem. Phys.* **1996**, *105*, 5618.

MA011348X